Food Chemistry 503 (2026) 147793

Contents lists available at ScienceDirect

Food Chemistry

journal homepage: www.elsevier.com/locate/foodchem

Fusarium proliferatum secondary metabolism: Multi-approach metabolomics insights

Irene Picicci [a], Mario Masiello [b], Antonia Susca [b], Antonio Moretti [b], Chiara Dall'Asta [a], Guillem Campmajó [a,*]

[a] Department of Food and Drug, University of Parma, Parma, Italy
[b] National Research Council of Italy, Institute of Sciences of Food Production, CNR-ISPA, Bari, Italy

ARTICLE INFO

Keywords:
Mycotoxins
Fusarium proliferatum
Metabolomics
High-resolution mass spectrometry
Feature-based molecular networking
Ion mobility
CCS

ABSTRACT

Fusarium proliferatum is a toxigenic filamentous fungus that produces the harmful mycotoxins fumonisins, contaminates worldwide a broad range of crops whose products are staple food, and consequently, poses a serious threat to both human and livestock health. However, metabolomic insights into its broader secondary metabolism remain limited. In this study, liquid chromatography–traveling wave ion mobility spectrometry–high-resolution mass spectrometry (LC–TWIMS–HRMS), combined with feature-based molecular networking (FBMN), was used to map *F. proliferatum* secondary metabolism. As a result, 111 metabolites were tentatively identified, including fumonisins their modified forms (i.e. hydrolysed, acylated, and bound derivatives), beauvericins, and other toxic metabolites, many of which are not routinely monitored, despite their putative toxicological significance. Among them, N-(deoxy-D-fructos-1-yl)-FB4 and two fumonisin A4 isomers are herein reported for the first time. Furthermore, the $^{TW}CCS_{N2}$ values of the *F. proliferatum* metabolites were experimentally determined, showing structural trends, and providing a valuable reference for future studies.

1. Introduction

Natural toxins are among the main causes of foodborne illnesses, globally compromising food safety and security (World Health Organization, 2015). Specifically, mycotoxins are low-molecular-weight secondary metabolites produced by toxigenic filamentous fungi (e.g. *Alternaria*, *Aspergillus*, *Fusarium*, or *Penicillium* spp.) in a wide range of food commodities at both pre- and post-harvest stages of the food chain. These compounds pose significant health risks upon consumption, ranging from acute toxicity to chronic effects such as nephrotoxicity, hormonal and reproductive disruption, developmental block, and even cancer (Goessens et al., 2024). As a result, authorities in several countries have established regulatory limits to control their presence in foodstuffs (Food and Drug Administration, 2000; The Commission of the European Communities, 2006).

Fusarium proliferatum is a toxigenic species of the genus *Fusarium*, belonging to *Fusarium fujikuroi* species complex (FFSC) (Munkvold et al., 2021). It is globally distributed and can infect a vast variety of hosts, including maize, rice, garlic, date palm, pine, and sugar cane (Proctor et al., 2010). Together with phylogenetically close *F. verticillioides*, this species is one of the most well-known producers of fumonisins, of which several structural analogues belonging to the A, B, C, and P series have been reported to date (Anumudu et al., 2025). Moreover, fumonisins are among the most widespread, hazardous, and therefore highly regulated mycotoxins. In particular, fumonisin B1 (FB1) is currently classified by the International Agency for Research on Cancer (IARC) as a Group 2 carcinogen in humans (World Health Organization. International Agency for Research on Cancer, 2002) and has been associated with an increased incidence of oesophageal and liver cancers (Yu et al., 2021). Therefore, within this context, fumonisins are of major concern in food systems due to their frequent occurrence not only in staple foods (such as cereal-based commodities) but also in a broad range of other food products, including fruits and vegetables, leading to widespread exposure (Li et al., 2024).

Additionally, *F. proliferatum* also synthesises other toxic metabolites (e.g. beauvericins, moniliformin, fusarins) along with a wide array of structurally distinct secondary metabolite families (e.g. bikaverins, prolipyrones) (Munkvold et al., 2021; Niehaus et al., 2016). The production of these toxic metabolites, combined with its notable adaptability, make this species one of the most important causes of

* Corresponding author.
E-mail address: guillem.campmajogalvan@unipr.it (G. Campmajó).

https://doi.org/10.1016/j.foodchem.2025.147793
Received 13 September 2025; Received in revised form 7 December 2025; Accepted 27 December 2025
Available online 28 December 2025

agricultural economic losses, a threat to food safety, and particularly critical to control in the current climate change scenario. In fact, a newly published study by Tagyan et al. (Tagyan et al., 2025) assesses how future global warming and high-emission scenarios could expand the range of *F. proliferatum* infections into new geographical regions, especially in temperate areas of the Northern Hemisphere, with major implications for global food safety.

Nevertheless, metabolomic insights into its secondary metabolism remain limited, and several compounds — even those related to fumonisins and other toxins' metabolism — are still unknown or uncharacterised. The main reason to this is that, in general, most studies on the metabolism of toxigenic filamentous fungi have focused on evaluating the production of their major mycotoxins through targeted liquid chromatography coupled to mass spectrometry (LC−MS) (Shi et al., 2017), thereby overlooking key insights into the fungal biology, the discovery of novel compounds, and their implications for food safety. Understanding the metabolism of these organisms and exploring their chemical diversity is both crucial and increasingly urgent — not only for monitoring mycotoxin contamination, but also for assessing how climate change may influence their biosynthesis — with the aim of developing effective surveillance strategies, while potentially identifying novel metabolites of technological interest.

In this context, liquid chromatography coupled to high-resolution mass spectrometry (LC−HRMS) — sometimes also combined with ion mobility spectrometry (IMS) — is an excellent instrumental platform for comprehensively expanding the coverage of fungal secondary metabolites, providing a broader and more detailed snapshot. Its high resolving power, great selectivity and sensitivity, and ability to provide structural information enable the tentative identification of both known and unknown compounds for which analytical standards are not available (Righetti et al., 2016). However, to date, few studies have exploited the potential of LC−HRMS to explore the metabolome of toxigenic filamentous fungi. For instance, Molnár et al. pointed out the metabolomic differences between *Alternaria alternata* and *Alternaria arborescens*, two of the most occurring species of *Alternaria* genus in wheat, through a non-targeted approach, identifying eight *Alternaria* mycotoxins (Molnár et al., 2023).

Furthermore, the use of non-targeted LC−HRMS data analysis methods, such as feature-based molecular networking (FBMN), which connects metabolites based on structural similarities, has enhanced the exploration and annotation of unknown molecules (Nothias et al., 2020). In this line, although FBMN has gained popularity in the plant metabolomics field (Damiani et al., 2025), its application within the mycotoxin research domain has so far been limited. Thus, FBMN is of particular interest in the fungal metabolomics field, as it facilitates the discovery of potential novel mycotoxin analogues whose parent compounds are already known, while providing structural context that enhances annotation confidence. Moreover, it also offers an effective way to prioritise metabolites of interest in non-targeted analyses. As an example, Witte et al. used FBMN to find dehydrocurvularin analogues produced by different *Alternaria* isolates (Witte et al., 2022).

To our knowledge, such comprehensive approach has not yet been applied with a specific focus on *F. proliferatum* secondary metabolism nor other *Fusarium* species. Therefore, the present study aimed to establish an analytical workflow based on a liquid chromatography−-traveling wave ion mobility spectrometry−high-resolution mass spectrometry (LC−TWIMS−HRMS) platform to decipher and map the secondary metabolism of *F. proliferatum*. In particular, it focused on: *i*) the reliable identification of the main *F. proliferatum* mycotoxins and other related relevant metabolites through targeted and suspect analysis using an in-house database; *ii*) the use of FBMN to enhance the molecular coverage of uncharacterized structurally related metabolites following a non-targeted approach; and *iii*) building a TWIMS-derived collision cross section ($^{TW}CCS_{N2}$) database for the identified compounds.

2. Materials and methods

2.1. Reagents and solutions

Purified water was obtained using a Milli-Q system (Millipore Corporation, Bedford, MA, USA). LC−MS grade water and methanol, as well as ammonium acetate and acetic acid (99.99 %), were supplied by Merck (Darmstadt, Germany). Methyl *tert*-butyl ether (MTBE) was from Carlo Erba (Milan, Italy).

The analytical standards used for identity confirmation were purchased from Romer Labs (Tulln) and consisted of FB1, FB2, FB3, and BEA.

2.2. Fusarium proliferatum strains and culture conditions

Thirteen *F. proliferatum* strains were included (ITEM18597, ITEM18601, ITEM18592, ITEM18611, ITEM18617, ITEM18640, ITEM18584, ITEM18621, ITEM18612, ITEM18596, ITEM18604, ITEM18605, ITEM18609, ITEM18620), aiming to represent the diverse FB1 production of this species on a single host, based on a previous study (Rabaaoui et al., 2021).

The strains were originally isolated on date palm (*Phoenix dactylifera*) in Tunisia, and subsequently molecularly identified and preserved in the CNR-ISPA-ITEM, Agri-food Microbial Collection of the Institute of Sciences of Food Production of the National Research Council in Bari (Institute of Sciences of Food Production, 2025). Strains isolated from the same geographical area and host plant were selected to minimize possible metabolic differences associated with these variables. For each strain, five mycelium plugs (4 mm), collected from the margin of actively growing colonies, were used to inoculate flasks containing 30 g of rice, previously hydrated to 45 % moisture with distilled water, and autoclaved at 121 °C for 30 min. Samples were cultivated in triplicate and incubated in the dark at 25 °C for 21 days. Rice cultures were then dried at 65 °C for 2 days. Not inoculated rice treated in the same way was used as negative control.

Rice was selected as the culture substrate because it provides a favourable C/N ratio for secondary metabolite production, as well as homogeneous water activity and temperature. Moreover, it exhibits minimal background contamination and noise and is commonly used in *Fusarium* research, facilitating comparability with existing literature (Rabaaoui et al., 2021).

2.3. Sample preparation and analysis

Rice samples were finely ground using the A10 basic bench-top lab mill from IKA (Staufen im Breisgau, Germany). Aliquots (25 mg) of the powder were then treated following the Salem et al. protocol (Salem et al., 2016), which consists of a biphasic solid-liquid extraction (SLE) using MTBE:methanol (3:1, *v/v*) and water:methanol (3:1, *v/v*) as the apolar and polar solutions, respectively. Briefly, after orbital shaking (HS 501 horizontal shaker, IKA), sonication (VWR ultrasonic cleaner, VWR International, Milan, Italy), and centrifugation (5810R centrifuge, Eppendorf, Hamburg, Germany), 400 µL of the polar phase were transferred into an Eppendorf vial and dried in a CentriVap centrifugal concentrator (Labconco, Kansas City, MO, USA). Each concentrated sample was finally re-suspended in a final volume of 200 µL methanol: water solution (1:1, *v/v*) and stored at −20 °C in small volume glass injection vials until analysis.

Regarding sample analysis, three main strategies were employed to assess instrumental performance and ensure the quality of the LC−TWIMS−HRMS data. First, randomization of the sample analysis order to minimize systematic bias. Second, use of a solvent blank sample, composed of the reconstitution mix, to monitor the background noise and control carryover. Third, preparation of a quality control (QC) sample by mixing equal aliquots of all the analysed samples to detect and correct potential instrumental drifts. Both solvent blank and QC

samples were periodically injected throughout the injection sequence.

2.4. Instrumentation

The LC was performed using an ACQUITY UPLC I-Class separation system (Waters, Wilmslow, UK). The chromatographic separation was conducted on an Acquity BEH C_{18} column (100 mm × 2.1 mm, 1.7 μm particle size) (Waters, Wilmslow, UK), using a mobile phase composed of a 1 mM ammonium acetate aqueous solution (solvent A) and methanol (solvent B), both acidified with 0.5 % (*v/v*) of acetic acid. The following multistep elution gradient program, adapted and modified from a previous study (Righetti et al., 2020), was applied: 0–1.0 min, isocratic elution at 5 % solvent B; 1.0–5.0 min, linear gradient up to 40 % B; 5.0–14.0, further increase to 95 % B; 14.0–15.0, isocratic elution at 95 %. Finally, initial conditions were set in 0.5 min and kept over 3.5 min for system re-equilibration. Overall, the proposed elution gradient resulted in an analysis time of 19 min. The column was maintained at 35 °C and the mobile phase flow rate was 0.3 mL·min^{-1}.

The chromatographic system was coupled to a Vion IMS-QTOF mass spectrometer (Waters, Wilmslow, UK) through a heated-electrospray ionisation (H-ESI) source, operated both in positive and negative modes. In this regard, each sample was injected twice to acquire data in both positive and negative ESI modes. Table S1 summarizes the established H-ESI parameters. For HRMS detection, the mass spectrometer operated using the sensitivity analyser mode and the high definition MS^E (HDMS^E) acquisition mode. Specifically, the HDMS^E combines full-scan MS and data independent acquisition (DIA) modes (*m/z* 50–1000), applying 5 V and a ramp from 27 to 45 V of collision energy, respectively. Furthermore, TWIMS was performed with a nitrogen flow rate of 25 mL·min^{-1}, and wave velocity and height of 300 m·s^{-1} and 15 V, respectively.

The Vion IMS-QTOF system was calibrated using the Major Mix IMS/ToF Calibration Kit (Waters, Wilmslow, UK) for both positive and negative modes, covering an approximate *m/z* range from 150 to 2000 and Å^2 range from 130 to 370. Additional details regarding the preparation of the CCS calibration solution, its composition, and the calibration procedure have been previously described by Aparicio-Muriana et al. (Aparicio-Muriana et al., 2023). In addition, leucine-enkephalin was infused at 10 μL·min^{-1} as the LockSpray solution (200 pg·μL^{-1}) for real-time *m/z* and CCS correction.

Samples were maintained at a constant temperature of 10 °C and a fixed injection volume (2 μL) of each sample was set for the analysis.

2.5. Data analysis

The UNIFI software (Waters, Manchester, UK) was used to control the LC−TWIMS−HRMS system and to acquire and process the data. Targeted and suspect analyses were performed in two consecutive steps: *i*) creation of a targeted and suspect compound list and *ii*) peak identification. The in-house list (see Table S2) comprised 51 mycotoxins (for which analytical standards were available) and 153 suspect compounds, consisting of secondary metabolites associated with the *Fusarium* genus, most of which are specific to the *F. proliferatum* species. Suspect metabolites were selected from online resources such as NPAtlas (Poynton et al., 2025) and MicotoXilico (Tolosa et al., 2023). Peak identification was carried out by the Metabolomics Standard Initiative guidelines (Schymanski et al., 2014). Both ESI positive — $[M]^+$, $[M+H]^+$, $[M+Na]^+$, $[M+K]^+$, $[M+NH_4]^+$ — and negative — $[M-H]^-$, $[M+Cl]^-$, $[M+CH_3COOH-H]^-$ — adduct forms were considered. The established acceptance criteria for HRMS identifications included mass error < 5 ppm, isotopic pattern fit > 80 % (isotope match error < 20 %), and MS^2 spectral similarity. For targeted compounds, experimental MS^2 data were compared with those of the analytical standards. Instead, for suspect metabolites, identification relied on literature data (Arndt et al., 2015; Bartók et al., 2006, 2010, 2013; Dall'Asta et al., 2008; Gasser et al., 2023; Kleigrewe et al., 2011; Matsuo et al., 2015; Seefelder et al., 2001; Seiferlein et al., 2007; Selegato et al., 2023; Urbaniak et al., 2019), public databases — mzCloud (HighChem LLC, Bratislava, Slovakia) and MassBank (Horai et al., 2010) —, or the in-silico fragmentation using MetFrag software (Wolf et al., 2010). Additionally, the identification of the targeted metabolites included the agreement on retention time (< 0.1 min) and $^{TW}CCS_{N2}$ (< 2 %) compared to the analytical standard.

The LC−TWIMS−HRMS data were also processed through a non-targeted approach using the Progenesis QI software (Waters, Manchester, UK). Thus, retention time alignment was first performed over the 0–15 min range. Peak picking was then carried out using the 'Sensitivity' algorithm with a minimum peak width of 0.05 min. Moreover, a 5 % base-peak-intensity cutoff was applied to filter out low-intensity fragments generated in HDMS^E mode. Finally, peak deconvolution was performed. The data were exported — '.csv' file containing feature intensities in each sample and '.msp' file with the MS/MS spectra — and subsequently handled with the GNPS2 environment for FBMN (Nothias et al., 2020) and Cytoscape 3.10.3 (Shannon et al., 2003) for network visualisation. For the creation of the molecular network, the precursor and fragment ion tolerances were both set at 0.02 Da. Moreover, edges between nodes indicated a cosine score above 0.7 and more than 4 matched fragments.

3. Results and discussion

A total of thirteen *F. proliferatum* strains inoculated in triplicate in rice were analysed by LC−TWIMS−HRMS. As an example, Fig. S1 depicts the total ion current (TIC) chromatograms obtained in positive and negative ESI modes for the QC, ITEM18592, and ITEM18621 samples. The analysis enabled the tentative identification of 111 *F. proliferatum* secondary metabolites: 103 were identified using the targeted and suspect approach, and 8 were identified through the non-targeted strategy. Table S3 summarizes the identified metabolites, providing several parameters related to their LC and HRMS acquisition. Overall, 4 compounds were annotated with identification confidence level 1, 37 at level 2, 67 at level 3, and 3 at level 4. Moreover, most of the evaluated metabolites were better ionised in positive ESI mode, with the protonated form $[M+H]^+$ being the most predominant adduct. Notably, only three compounds — i.e. fusarubin, prolipyrone A, and siccanol — exhibited better ionisation efficiency in negative ESI mode.

Fig. 1 depicts a pie chart categorising the identified *F. proliferatum* metabolites. Fumonisins were the predominant annotated class, accounting for 77.5 % of the total compounds described in this study. Beauvericins represented 9 %, bikaverins 4.5 %, and the remaining 9 % consisted of other secondary metabolites, spanning various chemical families.

3.1. Targeted and suspect analysis

As previously mentioned, most of the herein reported *F. proliferatum* metabolites (Table S3) were tentatively identified through targeted and suspect LC−TWIMS−HRMS analysis. The present section aims to provide a general outlook into the different chemical groups found.

3.1.1. Fumonisins

Numerous fumonisin analogues, including related structural isomers, were identified, representing all the major structural series described in the literature and produced by *F. proliferatum*. As expected, the most prevalent compounds corresponded to fumonisins belonging to the B-series (FBs), characterised by a C18 polyketide backbone, produced by a polyketide synthase (PKS) enzyme, and functionalised with two tricarballylic esters and an amino group derived from alanine. Fumonisin B1 (FB1), B2 (FB2), and B3 (FB3) were identified through targeted analysis using their analytical standards, serving as reference for RT, fragmentation patterns, and CCS to aid in the detection of additional fumonisin B analogues and isomers.

Instead, fumonisin B4 (FB4) and B5 (FB5) were screened by suspect

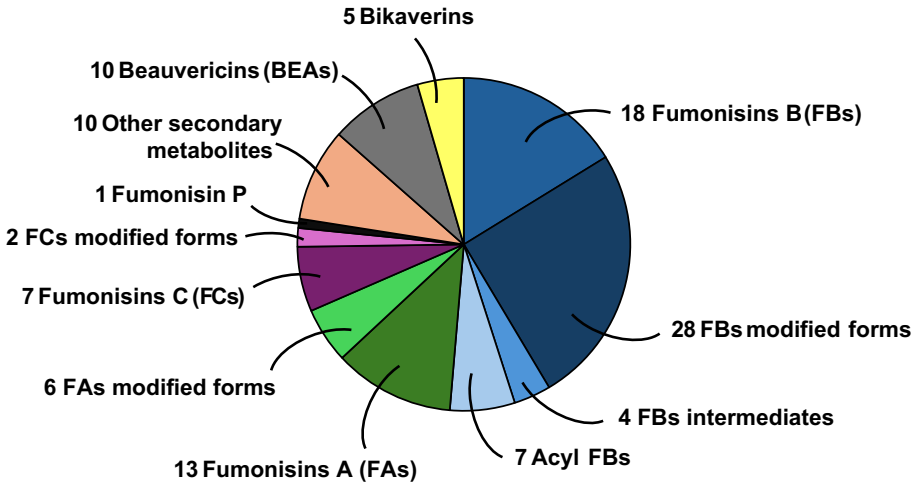

Fig. 1. Pie chart showing the different groups of metabolites tentatively identified in rice inoculated with *Fusarium proliferatum*.

analysis. Fig. S2 shows the HDMS^E fragmentation spectra that allowed the tentative identification of the major FBs. Interestingly, FB5 — an analogue structurally characterised by a hexahydroxyalkyl backbone — presented the highest number of isomers (10 in total) in our samples, consistent with prior observation in a *F. verticillioides*-inoculated rice culture (Bartók et al., 2013). Nevertheless, FB5 is a rarely reported fumonisin analogue, and its toxicological relevance is still poorly understood (Bartók et al., 2006; Musser & Plattner, 1997). Moreover, while FB1 and FB2 are known to be biosynthesised from FB3 and FB4, respectively, via enzymatic conversion by the dioxygenase FUM3 (Butchko et al., 2006), the biosynthesis of FB5 remains unclear.

Additionally, the suspect approach also enabled the tentative identification of isomers of 2-amino-14,15-dihydroxy-12,16-dimethylcosan-3-one and 2-amino-12,16-dimethylicosane-3,4,15-triol. Along with hydrolysed FB3, these are two FB1 and FB2 pathway intermediates and, therefore, their annotation could be of interest for future pathway analysis studies.

A-series fumonisins (FAs) were also produced by the *F. proliferatum* strains analysed in this study. In particular, fumonisin A1 (FA1) with seven isomers, fumonisin A2 (FA2) with one isomer, and fumonisin A3 (FA3) were detected. Fig. S3 displays the HDMS^E fragmentation spectra that enabled their tentative identification. These analogues share the same backbone as FBs but are acetylated at the amino group (Tamura et al., 2014). C-series analogues — fumonisin C1 (FC1), C2 (FC2), C3 (FC3), and C4 (FC4) — along with several of their isomers, were also annotated (see HDMS^E fragmentation data in Fig. S4). Structurally, these compounds lack the terminal C1 methyl groups. Besides, they are hypothesised to be produced in place of FB1 or FB2 from the alternative expression of a fum8 orthologue gene (Proctor et al., 2008). The production of these analogues was expected, as they have often been reported in various *Fusarium* species, specifically *F. proliferatum* (Lazzaro et al., 2013; Musser et al., 1995). Finally, fumonisin P1 (FP1) was the only member of the P-series detected. Fig. S5 contains the HDMS^E fragmentation spectrum that allowed its tentative annotation.

In summary, what primarily differentiates fumonisin analogues is their toxicity, which is strictly dependent on their structure. For example, while FCs are about as toxic as B-series fumonisins, FP1 appears to be less toxic to plants and mammalian cells. This reduced toxicity has been attributed to the replacement of the amino group with a 3-hydroxy-pyridine moiety (Abbas et al., 1998). Still, more toxicological data are needed, especially for the less-investigated analogues, to assess their risk better and develop potential detoxification strategies.

3.1.2. *Fumonisin modified forms*

In addition to the fumonisin analogues mentioned above, LC−TWIMS−HRMS enabled the tentative identification of 43 structurally modified forms (mainly from the B-series) such as hydrolysed, bound, acylated, or deaminated derivatives. These compounds are commonly referred to as 'masked mycotoxins', as their chemical differences from the parent forms often lead to escape detection. However, they may exert synergistic toxic effects in conjunction with their parent forms (Berthiller et al., 2015). In this regard, their inclusion in food safety assessments has been emphasised by the European Food Safety Authority (EFSA) (Knutsen et al., 2018; Nielsen et al., 2018), which also highlighted the need for additional exposure and toxicity data.

In this study, 11 hydrolysed fumonisins (HF) and 13 partially hydrolysed fumonisins (PHF) were annotated across the B-, A-, and C-series. In the B-series, while HFBs lack both tricarballylic side chains, PHFBs retain one resulting in differences in polarity and interactions with ceramide synthase involved in their toxicity (Renaud et al., 2021). For example, HFB1 exhibits lower affinity for ceramide synthase, yet it still disrupts sphingolipid metabolism to a certain extent (Dellafiora et al., 2018).

HF and PHF formation is often attributed to alkali treatments, usually related to food processing, but can also occur upon biotransformation by the gut microbiota, especially in pigs and poultry (Antonissen et al., 2020). Nonetheless, HFB3 is also a biosynthetic intermediate in the fumonisin pathway, produced by the FUM2 enzyme through hydroxylation at the C-10 position of the aforementioned 2-amino-12,16-dimethylicosane-3,4,15-triol (Kolawole et al., 2021).

Suspect screening also revealed the presence of bound fumonisins. For instance, *F. proliferatum* strains produced several isomers of N-(deoxy-D-fructos-1-yl)-FBs and N-(carboxymethyl)-FBs. These metabolites have been described as Maillard reaction products formed during processing (Seefelder et al., 2001) and have not previously been reported as fungal metabolic products. Some of these compounds may have formed via the Maillard reaction of the parent fumonisins during sample handling, as the rice cultures were subjected to a two-day drying treatment at 65 °C.

Collectively, these FBs modified forms (e.g., HFB, PHFB, N-(deoxy-D-fructos-1-yl)-FBs, or N-(carboxymethyl)-FBs) have been described as "chemically modified" mycotoxins formed during food processing (Rychlik et al., 2014). Their presence in the analysed samples warrants further investigation, as their origin remains unclear. Any endogenous fungal production should be confirmed using genomic or transcriptomic analyses of the same samples. Regardless of their origin, our method provided data on compounds that may co-occur with the parent

fumonisins and other toxic species in food, potentially contributing to a cumulative exposure or "cocktail" effect for consumers.

Likewise, seven fatty acid conjugated fumonisins — among which O-linoleoyl, O-palmitoyl, and O-oleoyl bound forms of FB1 — were tentatively identified. Their detection is consistent with previous reports in *F. verticillioides* cultures on maize-based substrates (Falavigna et al., 2016). The identification of the O-acylated FBs is of particular importance since emerging evidence indicates that some of these lipophilic derivatives form highly stable complexes with human serum albumin (HSA) and exhibit enhanced in vivo toxicity. Specifically, Csenki et al. found that 5-O-palmitoyl-FB1 strongly interacted with HSA, inducing severe developmental defects, teratogenic effects, and up to 30 % mortality in zebrafish embryos after 24 h exposure at a 200 μM concentration (Csenki et al., 2023). The concomitant presence of the O-acylated forms of different B-series fumonisins (e.g. O-palmitoyl, O-linoleoyl, or O-oleoyl FB2/B3 isomers) in *F. proliferatum* cultures — whether formed by interaction with the lipid composition of the rice substrate or by fungal metabolism — raises new questions regarding their toxicity, co-occurrence relevance, and associated risks to human health.

Finally, fumonisin Py2 (FPy2) and Py4 (FPy4), the deaminated forms of FB2 and FB4 respectively, were also annotated. These forms show a reduced toxicological activity compared to FBs due to the loss of the amine moiety (Renaud et al., 2021). Several studies have focused on characterising the enzyme responsible for their formation, as part of enzymatic detoxification strategies purposes (Burgess et al., 2016; Garnham et al., 2020). To date, both molecules have only been reported in *Aspergillus welwitschiae* and *A. niger* but not in *Fusarium* species, in which such an enzymatic activity still remains undetected. The presence of FPy2 and FPy4 in the analysed samples warrants further investigation. It is not clear whether these forms are produced by *F. proliferatum* through uncharacterised enzymatic activities analogous to those reported in the two *Aspergillus* species, or whether they merely represent abiotic derivatives of the parent toxin. More in-depth studies integrating genomic and transcriptomic data may be required to clarify this point.

3.1.3. Beauvericins

Beauvericin (BEA) was identified at the identification confidence level 1, using its analytical standard. In addition, seven of its analogues were annotated through suspect analysis. BEAs are non-ribosomal hexacyclic depsipeptides, composed of three alternating D-2-hydroxyisovaleric acid and three N-methyl-*L*-amino acid residues. All the above-mentioned BEA analogues — except for beauvenniatin A — have been previously reported in *F. proliferatum* strains (Gálvez et al., 2017; Logrieco & Moretti, 1995; Urbaniak et al., 2020; T. Zhang et al., 2013). Beauvenniatin A, however, may be of particular interest for investigating novel non-ribosomal peptide synthase (NRPS) enzymatic activities in this species.

Interestingly, the name beauvericin K has been associated with compounds with different molecular formulas in previous studies: $C_{42}H_{59}N_3O_9$ and $C_{45}H_{57}N_3O_{11}$ (Urbaniak et al., 2019; Xu et al., 2016). Herein, we indicate these metabolites as beauvercin K and beauvericin K′, respectively, based on the date of publication. This fact highlights the complexity of identifying this class of compounds and indicates the need to explore further and resolve the structures of BEA analogues.

Indeed, BEAs, together with enniatins, beauvenniatins, and moniliformin, are considered 'emerging' mycotoxins and still lack regulatory limits, further toxicological investigations are warranted. A very recent EFSA opinion addressed BEA genotoxicity, but comprehensive risk assessments remain incomplete (Knutsen et al., 2024).

3.1.4. Bikaverins

Five bikaverin-related metabolites were detected and annotated in this study. Bikaverin is a polyketide pigment commonly reported in *F. oxysporum* and members of the *F. fujikuroi* species complex (Lale & Gadre, 2016; Limón et al., 2010; Santos et al., 2020). Once regarded solely as a mycotoxin, bikaverin has since shown diverse biological activities, including pathogenic effects on plants, antibiotic activity against various microorganisms, and even antitumoral properties (Deshmukh et al., 2014; Lu et al., 2025), prompting growing interest in its biotechnological applications.

Notably, transcripitional factors affecting both bikaverin and fumonisin biosynthesis suggest regulatory cross-talk between their pathways (Lazzaro et al., 2012). For instance, recently, CRISPR-Cas9-mediated deletion of bikaverin biosynthetic genes impacted the production of other polyketide metabolites, likely through modulation of acetyl-CoA pools (Huang et al., 2025). The annotation of biosynthetic intermediates in this study could inform future research into these regulatory mechanisms.

3.1.5. Other secondary metabolites

Finally, in addition to the major classes described above, several metabolites were identified, belonging to diverse chemical families and not falling under the fumonisins, beauvericins, or bikaverins. Thus, they are here classified as 'other secondary metabolites'. In detail, these compounds include prolipyrone A and B, gibepyrone D, fusarubin, siccanol, fusaproliferin, three isomers of fusarin C, and sambutoxin.

Fusarin C and fusaproliferin are toxic fungal metabolites classified among the so-called 'emerging mycotoxins' (Jestoi, 2008). These compounds have been previously reported in *F. proliferatum* and other *Fusarium* spp. (Ćeranić et al., 2021; Jajić et al., 2019; Moretti et al., 1996). Siccanol, also referred to as terpestacin, is a fusaproliferin-derived metabolite with reported phytotoxic and antimicrobial properties (Chan & Jamison, 2004). Sambutoxin, a seldom-reported tetrahydrofuran derivative originally isolated from *F. sambucinum*, has demonstrated cytotoxic and hemorrhagic effects (Abbas et al., 2001). While being recently reported in cultures of *F. avenaceum*, (Witte et al., 2024), to our knowledge, data on sambutoxin production in *F. proliferatum* are missing.

3.2. Feature-based molecular networking (FBMN) analysis

Furthermore, non-targeted analysis was also performed to detect and identify unconsidered or unknown metabolites structurally related to those found via the targeted and suspect approaches. To that end, FBMN, which connects molecules based on similarities in their fragmentation data, was performed on the 4739 features derived from the ESI positive LC−TWIMS−HRMS raw data after processing with Progenesis QI (Waters, Manchester, UK). As a result, Fig. S6 shows the obtained global molecular network.

It is important to note that the $HDMS^E$ acquisition method was selected because, as a DIA mode, it enables fragmentation of all ions within a specific m/z range, including low-abundance metabolites. Furthermore, the additional TWIMS dimension enhances the MS^2 spectral quality through ion mobility filtering, thereby improving fragment-to-precursor assignment. However, coeluting species with similar mobility may inevitably interfere; therefore, several steps were implemented when dealing with the resulting MNs to address this issue.

As an example, Fig. S7 provides a schematic illustration of the steps followed to detect the unknown fumonisin- and beauvericin-related metabolites. First, the metabolites identified through the targeted and suspect approaches were mapped onto the global molecular network. Particular attention was then directed to the MNs that contained them. Second, nodes were grouped based on their retention time (RT), revealing the presence of several coeluting ions, which could correspond to the same molecular feature or to interferences resulting from the use of DIA mode. Third, node size was scaled according to their relative intensity compared to the coeluting ions, with the aim of identifying the precursor ion in each case. Moreover, each node was represented as a pie chart based on its abundance across the various FB1 production groups (FB producer, low-producer, and non-producer), although the chemical and biological interpretation of these results falls beyond the scope of the present study. Finally, tentative annotation of the unidentified nodes

was carried out using UNIFI (Waters, Manchester, UK), MetFrag (Wolf et al., 2010), and literature resources.

Fig. 2 depicts the three main MNs were the already identified *F. proliferatum* metabolites were clustered. Among them, two (MN1 and MN2) were related to fumonisins and one to beauvericins (MN3). For instance, MN1 was made up of 60 nodes and contained six identified fumonisins such as fumonisin B1, fumonisin B2, and N-(deoxy-D-fructos-1-yl)-FB1, among others. Unidentified metabolites in MN1 included *m/z* 890.4346 $[M+Na]^+$ (RT 10.22 min), 890.4345 $[M+Na]^+$ (RT 10.95 min), and 874.4397 $[M+Na]^+$ (RT 11.55 min), and were putatively annotated as N-(deoxy-D-fructos-1-yl)-FB3, N-(deoxy-D-fructos-1-yl)-FB2, and N-(deoxy-D-fructos-1-yl)-FB4, respectively. In this regard, while the existence of the formers had been previously reported in corn by Matsuo et al. (Matsuo et al., 2015), this is the first time that N-(deoxy-D-fructos-1-yl)-FB4 is detected to our knowledge. Its $HDMS^E$ fragmentation spectrum is reported in Fig. S8. Instead, only the molecular formula could be assigned to *m/z* 812.4022 $[M+Na]^+$ (RT 10.30 min), referred as Unknown 1.

MN2 contained 72 nodes among which fumonisin B4, several A-series fumonisins (i.e. fumonisin A1 isomer, fumonisin A2, fumonisin A3), and partially hydrolysed fumonisin A2/A3 isomer. The ion corresponding to *m/z* 732.4179 $[M+H]^+$ (RT 12.55 min) was tentatively identified as an isomer of fumonisin A4, being the first time that this A-series fumonisin analogue is described. In addition, retrospective analysis allowed the annotation of another fumonisin A4 isomer at RT 11.84 min. Their $HDMS^E$ fragmentation spectra are displayed in Fig. S8.

Finally, 24 nodes constituted MN3, which contained beauvericin-related metabolites. Aside from the beauvericin forms already identified through the suspect approach (beauvericin, beauvericin J, beauvericin J isomer, beauvericin A/F, and beauvericin K'), two unknown metabolites were also observed in the network. In this regard, Unknown 2 — *m/z* 792.3502 $[M+Na]^+$ (RT 12.29 min) — and Unknown 3 — *m/z* 785.4153 $[M+H]^+$ (RT 12.99 min) — were tentatively annotated with the molecular formulas $C_{40}H_{55}N_3O_{10}S$ and $C_{41}H_{57}N_3O_9S$, respectively. Interestingly, Selegato et al., who investigated the beauvericin production of *F. oxysporum* in Czapek broth using FBMN combined with Mass Spec Query Language, previously observed Unknown 2 clustering within the same molecular network as other beauvericin analogues. The authors hypothesised that this compound corresponded to a beauvericin analogue containing a methionine sulfoxide residue (Selegato et al., 2023).

3.3. Collision cross section (CCS) collection

It is well known that CCS has demonstrated to be an excellent chemical descriptor to be used as an additional parameter in compound identification, due to its matrix- and platform-independence (Celma et al., 2024). Despite the availability of several databases and CCS prediction tools, there is still very limited data, especially with regard to fungal metabolites.

In this context, the experimental $^{TW}CCS_{N2}$ values of the *F. proliferatum* metabolites were collected, considering the adducts observed in both positive and negative ionisation modes. Thus, Table S4 contains the $^{TW}CCS_{N2}$ measurements obtained for the 111 *F. proliferatum* metabolites identified, comprising a total of 382 ions. In particular, 272 ions — including 109 protonated, 93 sodium, 50 potassium, and 20 ammonium adducts — were found in the positive mode, covering a *m/z* range from 195 to 991 and a CCS range from 142.80 to 334.77 $Å^2$.

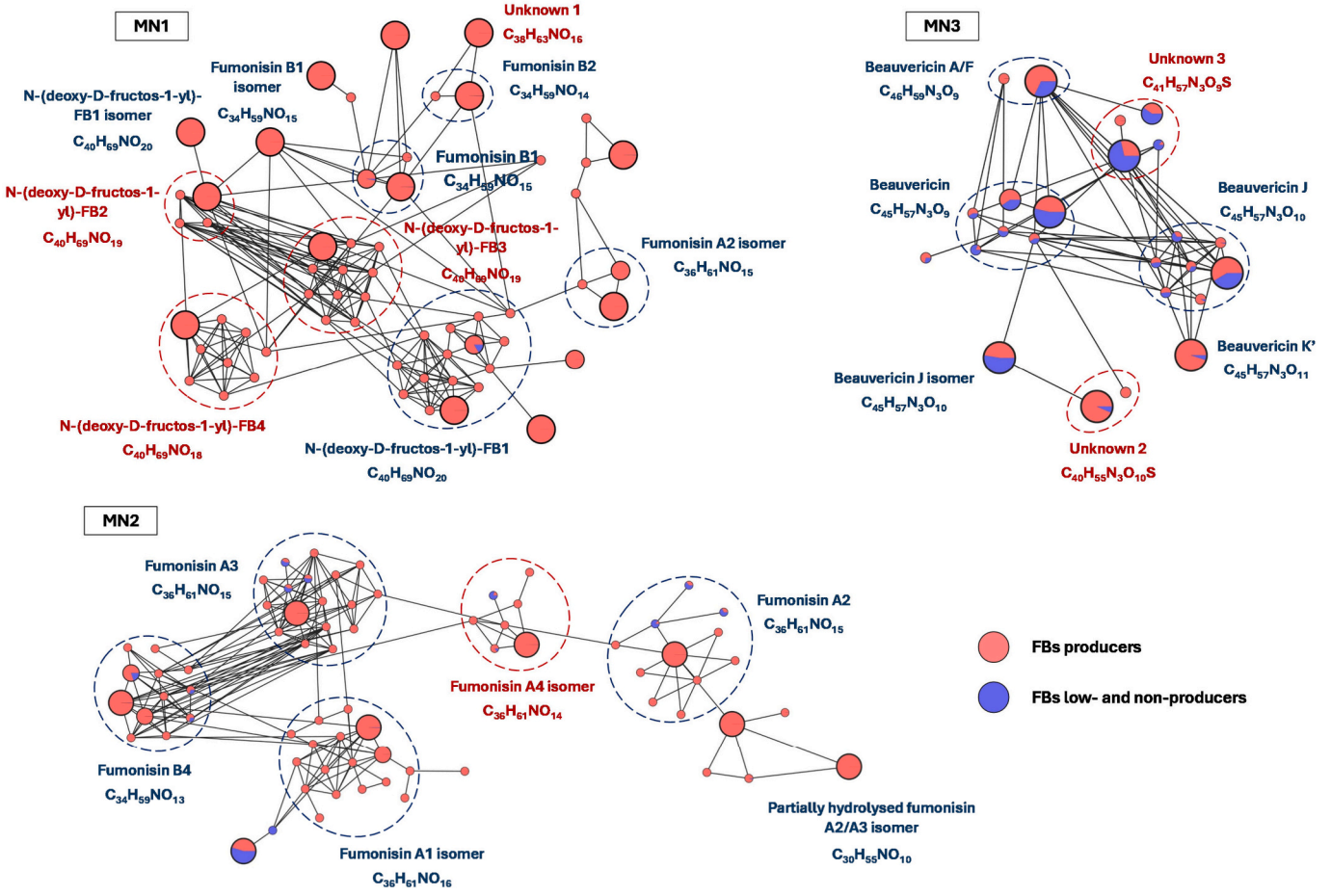

Fig. 2. Fumonisin- (MN1 and MN2) and beauvericin- (MN3) related molecular networks observed in the FBMN.

Instead, 110 ions — 92 deprotonated, 6 chloride, and 12 acetate adducts — were detected in the negative mode, covering a *m/z* range from 209 to 985 and a CCS range from 157.67 to 331.80 Å^2. Fig. 3 displays the $^{TW}CCS_{N2}$ vs. *m/z* for the protonated and deprotonated adducts identified as *F. proliferatum* secondary metabolites.

It is noteworthy that the $^{TW}CCS_{N2}$ values were collected from all the analysed samples in which the metabolites (and their corresponding adducts) were detected, resulting in variability in their abundance and a number of measurements (n) ranging from 5 to 52. As shown in Table S4, all ions presented a repeatability RSD below 2 %, with 63.4 % of them showing an RSD lower than 0.5 %, and 30.1 % with values between 0.5 % and 1 %.

As previously mentioned, Fig. 3 displays the $^{TW}CCS_{N2}$ vs. *m/z* plots for the protonated and deprotonated ions, detected in the positive and negative ESI modes, respectively. In both cases, four distinct groups were observed. First, fumonisin-related compounds (i.e. fumonisins, their modified forms, and pathway intermediates), which constituted the largest group of compounds, presented a strong correlation between $^{TW}CCS_{N2}$ and *m/z* for both protonated ($r = 0.9923$) and deprotonated ions ($r = 0.9870$). Second, acyl fumonisins did not follow this trend, exhibiting larger $^{TW}CCS_{N2}$ values due to the addition of linear acyl groups. Third, BEAs displayed higher $^{TW}CCS_{N2}$ values than several fumonisin forms within a similar *m/z* range, which may be attributed to the rigidity of their large macrocyclic ring structures. Finally, bikaverins showed lower $^{TW}CCS_{N2}$ values compared to other metabolites and did not align with any specific trend, possibly due to their cyclic and more compact structure. Metabolites classified as 'other secondary metabolites' could not be assigned to a specific trend due to the chemical diversity within this group.

Furthermore, of the 41 *F. proliferatum* metabolites identified at level 1 or 2 in the present study, the $^{TW}CCS_{N2}$ values for nine of them (i.e. BEA, FB1, FB2, FB3, FB4, HFB1, HFB2, HFB3, and N-(deoxy-D-fructos-1-yl)-FB1) had been reported in previous studies, involving different TWIMS platforms (Righetti et al., 2018, 2020). To verify the validity of the acquired $^{TW}CCS_{N2}$ values, and as an additional step beyond system calibration, these values were compared with those previously reported in these studies. As a result, Table S5 contains the obtained CCS deviations (ΔCCS, %). In most cases, errors below the acceptable CCS reproducibility threshold (±2 %) were obtained. In particular, 28 out of 32 ions presented a relative error below 2 %, with 25 of them exhibiting errors below 1 %.

The $[M+K]^+$ adduct of fumonisin B4 was among the four ions with ΔCCS >2 %, showing a slightly higher value of 2.09 %. The remaining three ions corresponded to the $[M-H]^-$ ions of hydrolysed fumonisins B1, B2, and B3, with ΔCCS equal to 4.93, 4.57, and 6.37 %, respectively. Interestingly, ΔCCS below 0.52 % were observed when comparing the experimental $^{TW}CCS_{N2}$ $[M-H]^-$ values of these hydrolysed fumonisin forms with their $^{TW}CCS_{N2}$ $[M+CH_3COOH-H]^-$ reference values. This may be because these forms ionise predominantly as $[M+CH_3COOH-H]^-$, are subsequently separated by ion mobility, and then fragmented to $[M-H]^-$ in the collision cell due to the low collision energy applied (5 V) in full-scan MS mode. Therefore, although the $[M-H]^-$ ions are detected for these hydrolysed forms, the measured $^{TW}CCS_{N2}$ values correspond to their $[M+CH_3COOH-H]^-$ precursors.

Furthermore, CCS vs. *m/z* trendlines — typically observed for compounds belonging to the same chemical family — have gained interest in recent years for enhancing confidence in compound identification (Celma, 2023; Schneiders et al., 2025). With this aim, three different approaches were tested to evaluate the CCS vs. *m/z* trendline for fumonisin-related compounds (see Fig. 3). Specifically, the approaches involved generating the fumonisin trendline for $[M+H]^+$ and $[M-H]^-$ using: *i*) previously existing experimental data (Righetti et al., 2018, 2020), *ii*) CCSbase predictions (Ross et al., 2020), and *iii*) AllCCS2 predictions (H. Zhang et al., 2023), and evaluating the fitness of our experimental data. A ± 3 % error margin was applied in each approach. The reference CCS values for the eight fumonisin-related compounds used in the first approach are listed in Table S5, whereas the predicted CCS data from CCSbase and AllCCS2 are presented in Table S6.

On the one hand, Fig. 4 presents the results obtained for the $^{TW}CCS_{N2}$ $[M+H]^+$ vs. *m/z* fumonisin trendline. Satisfactory fitting was obtained using the first approach, with most of the measured $^{TW}CCS_{N2}$ $[M+H]^+$ values being within the ±3 % margins of the trendline built using existing literature data. Moreover, although the two predictive tools are trained using data from different ion mobility platforms (i.e., drift tube and traveling wave ion mobility), the measured $^{TW}CCS_{N2}$ $[M+H]^+$ data fit perfectly the ±3 % thresholds established using the AllCCS2 predicted values, whereas a poor fit was observed with the CCSbase predictions. Indeed, the AllCCS2 predicted data offered the best performance among the three tested strategies, likely due to the limited amount of experimental data available in the literature and used in the first approach. Both approaches enhanced fumonisin-related compounds identification confidence.

On the other hand, Fig. S9 shows the results obtained for $^{TW}CCS_{N2}$ $[M-H]^-$ vs. *m/z* fumonisin trendline. In this case, poorer trendline fitting was observed across all three approaches. Remarkably, the goodness of fit varied along the *m/z* range. Specifically, satisfactory fitting was observed for metabolites with *m/z* above 650 using experimental literature data and CCSbase predicted values (AllCCS2 values did not provide a good fit in this range), while metabolites with *m/z* below 650 showed bad fit in all cases. As shown in Fig. S9, the $^{TW}CCS_{N2}$ $[M-H]^-$ values of some low-*m/z* metabolites — particularly certain hydrolysed and partially hydrolysed fumonisins — exceeded the upper limit of the

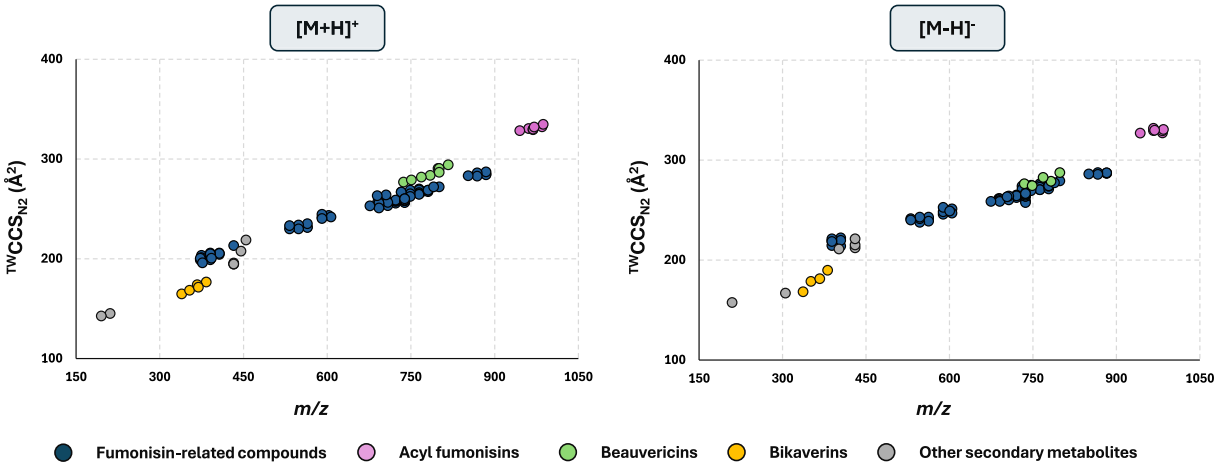

Fig. 3. $^{TW}CCS_{N2}$ vs. *m/z* for the protonated and deprotonated ions identified as *Fusarium proliferatum* metabolites.

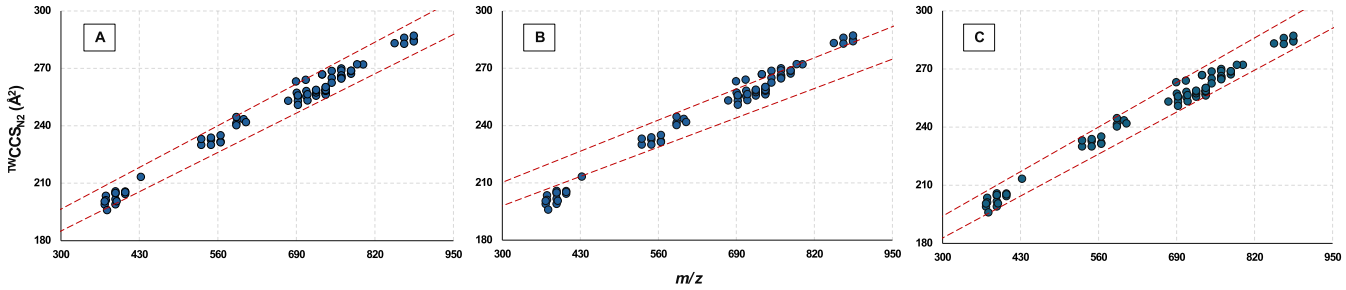

Fig. 4. Fitting of experimental CCS $[M+H]^+$ values for fumonisin-related compounds to trendlines generated from (A) previous experimental data, (B) CCSbase predictions, and (C) AllCCS2 predictions. Red dashed lines indicate the corresponding ±3 % deviation in each case. (For interpretation of the references to colour in this figure legend, the reader is referred to the web version of this article.)

three proposed strategies, suggesting a potential overestimation. This observation is consistent with the aforementioned comparison of $^{TW}CCS_{N2}$ values with previous studies. Indeed, these results support the hypothesis that the detected $[M-H]^-$ ions for some of these metabolites originate in the collision cell from the $[M+CH_3COOH-H]^-$ adduct due to the low energy applied for the full-scan MS mode; consequently, the measured $^{TW}CCS_{N2}$ values correspond to their $[M+CH_3COOH-H]^-$ precursors. The cases in which this may be occurring have been indicated in Table S4.

In summary, although CCS values are highly dependent on both the calibration mix and the instrumental system (further interplatform validation is required), and despite the tentative nature of the identification carried out, the TWIMS data provided in this study extend the characterisation of *F. proliferatum* mycotoxins and modified forms and could be used as reference in future studies. In this regard, the differing performance of the predictive tools, depending on the adduct monitored, for generating the CCS trendline highlights the need for experimentally obtained CCS databases. For instance, the $^{TW}CCS_{N2}$ vs. *m/z* fumonisin trendline could be used in future studies not only to strengthen the compound identification step but also as a potential tool for feature prioritisation in non-targeted analysis.

4. Conclusions

A multi-approach-based analytical workflow was applied to map the secondary metabolome of *F. proliferatum*, providing a broader perspective on its toxic potential. This strategy enabled the tentative identification of 111 metabolites — comprising B-, A-, C-, and P-series fumonisins, as well as hydrolysed, acylated, and bound derivatives — many of which are not routinely monitored despite their putative toxicological significance. Additionally, other secondary metabolite families were also annotated, including beauvericins, bikaverins, and other emerging toxins, such as fusarin C and fusaproliferin.

The use of FBMN enabled the clustering of structurally related metabolites and facilitated the annotation of previously unreported fumonisin and analogues. In particular, N-(deoxy-D-fructos-1-yl)-FB4 and two isomers of fumonisin A4 were herein reported for the first time. Additionally, the construction of a $^{TW}CCS_{N2}$ database adds a valuable dimension for future metabolite identification, especially for those lacking analytical standard.

The detection of such a wide array of structurally diverse forms underlines the importance of monitoring a broader range of toxins when *F. proliferatum* contamination is suspected. Coupling these data with genomics or transcriptomics insights could be key to resolving fundamental aspects of this species' metabolism, from uncharacterised enzymatic activities to whole biosynthetic pathways.

All in all, these findings highlight significant gaps in toxicological data required for proper risk assessment and the setting of regulatory limits on overlooked fumonisins forms and emerging toxins, which may not be detected but appear to be highly occurring. Results support a shift from target-only mycotoxin monitoring toward a more integrated metabolomic surveillance framework, especially in light of the ongoing environmental alterations and agricultural challenges driven by climate change.

Finally, these data, once more, underline the biodiversity of this fungal species, provided of an impressive amount of biochemical weapons that makes it among the most harmful species of the *Fusarium* genus.

CRediT authorship contribution statement

Irene Picicci: Writing – original draft, Methodology, Investigation, Formal analysis, Conceptualization. **Mario Masiello:** Investigation. **Antonia Susca:** Supervision, Resources, Conceptualization. **Antonio Moretti:** Writing – review & editing, Supervision, Resources, Funding acquisition, Conceptualization. **Chiara Dall'Asta:** Writing – review & editing, Supervision, Resources, Project administration, Funding acquisition, Conceptualization. **Guillem Campmajó:** Writing – original draft, Methodology, Investigation, Formal analysis, Conceptualization.

Fundings

The work was funded by the European Union under the project MYMATCH (grant agreement 101181208). G. Campmajó is holder of a Research Contract at the University of Parma, funded by the European Union – NextGenerationEU CUP D93C25000320006.

Declaration of competing interest

The authors declare that they have no known competing financial interests or personal relationships that could have appeared to influence the work reported in this paper

Acknowledgements

This work has been carried out in the frame of the ALIFAR project, funded by the Italian Ministry of University through the program 'Dipartimenti di Eccellenza 2023-2027'.

Appendix A. Supplementary data

Supplementary data to this article can be found online at https://doi.org/10.1016/j.foodchem.2025.147793.

Data availability

Data will be made available on request.

References

Abbas, H. K., Gronwald, J. W., Plaisance, K. L., Paul, R. N., & Lee, Y. W. (2001). Histone deacetylase activity and phytotoxic effects following exposure of duckweed (Lemna pausicostata L.) to Apicidin and HC-toxin. *Biochemistry and Cell Biology, 91*(12), 1141–1148.

Abbas, H. K., Shier, W. T., Seo, J. A., Lee, Y. W., & Musser, S. M. (1998). Phytotoxicity and cytotoxicity of the fumonisin C and P series of mycotoxins from Fusarium spp. fungi. *Toxicon, 36*(12), 2033–2037.

Antonissen, G., De Baere, S., Novak, B., Schatzmayr, D., Den Hollander, D., Devreese, M., & Croubels, S. (2020). Toxicokinetics of hydrolyzed fumonisin B1 after single oral or intravenous bolus to broiler chickens fed a control or a fumonisins-contaminated diet. *Toxins, 12*, 413. https://doi.org/10.3390/toxins12060413

Anumudu, C. K., Ekwueme, C. T., Uhegwu, C. C., Ejileugha, C., Augustine, J., Okolo, C. A., & Onyeaka, H. (2025). A review of the mycotoxin family of Fumonisins, their biosynthesis, metabolism, methods of detection and effects on humans and animals. *In International Journal of Molecular Sciences, 26*, 184. Multidisciplinary digital publishing institute (MDPI) https://doi.org/10.3390/ijms26010184.

Aparicio-Muriana, M. M., Bruni, R., Lara, F. J., del Olmo-Iruela, M., Hernandez-Mesa, M., García-Campaña, A. M., … Righetti, L. (2023). Implementing the use of collision cross section database for phycotoxin screening analysis. *Journal of Agricultural and Food Chemistry, 71*, 10178–10189. https://doi.org/10.1021/acs.jafc.3c01060

Arndt, B., Studt, L., Wiemann, P., Osmanov, H., Kleigrewe, K., Köhler, J., Krug, I., Tudzynski, B., & Humpf, H.-U. (2015). Genetic engineering, high resolution mass spectrometry and nuclear magnetic resonance spectroscopy elucidate the bikaverin biosynthetic pathway in fusarium fujikuroi. *Fungal Genetics and Biology, 84*, 26–36. https://doi.org/10.1016/j.fgb.2015.09.006

Bartók, T., Szécsi, Á., Szekeres, A., Mesterházy, Á., & Bartók, M. (2006). Detection of new fumonisin mycotoxins and fumonisin-like compounds by reversed-phase high-performance liquid chromatography/electrospray ionization ion trap mass spectrometry. *Rapid Communications in Mass Spectrometry, 20*, 2447–2462. https://doi.org/10.1002/rcm.2607

Bartók, T., Tölgyesi, L., Szécsi, Á., Varga, J., Bartók, M., Mesterházy, Á., Gyimes, E., & Véha, A. (2013). Identification of unknown isomers of fumonisin B5 mycotoxin in a fusarium verticillioides culture by high-performance liquid chromatography/electrospray ionization time-of-flight and ion trap mass spectrometry. *Journal of Liquid Chromatography and Related Technologies, 36*, 1549–1561. https://doi.org/10.1080/10826076.2012.692151

Bartók, T., Tölgyesi, L., Szekeres, A., Varga, M., Bartha, R., Szécsi, Á., Bartók, M., & Mesterházy, Á. (2010). Detection and characterization of twenty-eight isomers of fumonisin B1 (FB1) mycotoxin in a solid rice culture infected with fusarium verticillioides by reversed-phase high-performance liquid chromatography/electrospray ionization time-of-flight and ion trap mass spectrometry. *Rapid Communications in Mass Spectrometry, 24*, 35–42. https://doi.org/10.1002/rcm.4353

Berthiller, F., Maragos, C. M., & Dall'Asta, C. (2015). Introduction to masked mycotoxins. In C. Dall'Asta, & F. Berthiller (Eds.), *Masked mycotoxins in food: Formation, occurrence and toxicological relevance* (pp. 1–13). Royal Society of Chemistry. www.rsc.org.

Burgess, K. M. N., Renaud, J. B., McDowell, T., & Sumarah, M. W. (2016). Mechanistic insight into the biosynthesis and detoxification of Fumonisin mycotoxins. *ACS Chemical Biology, 11*, 2618–2625. https://doi.org/10.1021/acschembio.6b00438

Butchko, R. A. E., Plattner, R. D., & Proctor, R. H. (2006). Deletion analysis of FUM genes involved in tricarballylic ester formation during fumonisin biosynthesis. *Journal of Agricultural and Food Chemistry, 54*, 9398–9404. https://doi.org/10.1021/jf0617869

Celma, A. (2023). The use of ion mobility separation as an additional dimension for the screening of organic micropollutants in environmental samples. In M. López de Alda, C. Postigo, & B. Žonja (Eds.), *Vol. 138. Screening of pollutants in the environment. The handbook of environmental chemistry*. Springer. https://doi.org/10.1007/698_2023_1055.

Celma, A., Alygizakis, N., Belova, L., Bijlsma, L., Fabregat-Safont, D., Menger, F., & Gil-Solsona, R. (2024). Ion mobility separation coupled to high-resolution mass spectrometry in environmental analysis – Current state and future potential. In , *Vol. 43. Trends in environmental analytical chemistry*. Elsevier B.V, Article e00239. https://doi.org/10.1016/j.teac.2024.e00239.

Ćeranić, A., Svoboda, T., Berthiller, F., Sulyok, M., Samson, J. M., Güldener, U., … Adam, G. (2021). Identification and functional characterization of the gene cluster responsible for fusaproliferin biosynthesis in fusarium proliferatum. *Toxins, 13*, 468. https://doi.org/10.3390/toxins13070468

Chan, J., & Jamison, T. F. (2004). Enantioselective synthesis of (−)-terpestacin and structural revision of siccanol using catalytic stereoselective fragment couplings and macrocyclizations. *Journal of the American Chemical Society, 126*, 10682–10691. https://doi.org/10.1021/ja0470968

Csenki, Z., Bartók, T., Bock, I., Horváth, L., Lemli, B., Zsidó, B. Z., … Poór, M. (2023). Interaction of Fumonisin B1, N-Palmitoyl-Fumonisin B1, 5-O-Palmitoyl-Fumonisin B1, and Fumonisin B4 mycotoxins with human serum albumin and their toxic impacts on zebrafish embryos. *Biomolecules, 13*, 755. https://doi.org/10.3390/biom13050755

Dall'Asta, C., Galaverna, G., Aureli, G., Dossena, A., & Marchelli, R. (2008). A LC/MS/MS method for the simultaneous quantification of free and masked fumonisins in maize and maize-based products. *World Mycotoxin Journal, 1*(3), 237–246. https://doi.org/10.3920/wmj2008.x040

Damiani, T., Smith, J., Hebra, T., Perković, M., Čičak, M., Kadlecová, A., Rybka, V., Dračínský, M., & Pluskal, T. (2025). Computational metabolomics reveals overlooked chemodiversity of alkaloid scaffolds in Piper fimbriulatum. *The Plant Journal, 121*, Article e70086. https://doi.org/10.1111/tpj.70086

Dellafiora, L., Galaverna, G., & Dall'Asta, C.. (2018). Mechanisms of Fumonisin B1 toxicity: A computational perspective beyond the ceramide synthases inhibition. *Chemical Research in Toxicology, 31*, 1203–1212. https://doi.org/10.1021/acs.chemrestox.8b00188

Deshmukh, R., Mathew, A., & Purohit, H. J. (2014). Characterization of antibacterial activity of bikaverin from fusarium sp. HKF15. *Journal of Bioscience and Bioengineering, 117*(4), 443–448. https://doi.org/10.1016/j.jbiosc.2013.09.017

Falavigna, C., Lazzaro, I., Galaverna, G., Dall'Asta, C., & Battilani, P. (2016). Oleoyl and linoleoyl esters of fumonisin B1 are differently produced by fusarium verticillioides on maize and rice based media. *International Journal of Food Microbiology, 217*, 79–84. https://doi.org/10.1016/j.ijfoodmicro.2015.10.013

Food and Drug Administration. (2000). *Guidance for Industry: Action Levels for Poisonous or Deleterious Substances in Human Food and Animal Feed*.

Gálvez, L., Urbaniak, M., Waśkiewicz, A., Stępień, Ł., & Palmero, D. (2017). Fusarium proliferatum – Causal agent of garlic bulb rot in Spain: Genetic variability and mycotoxin production. *Food Microbiology, 67*, 41–48. https://doi.org/10.1016/j.fm.2017.05.006

Garnham, C. P., Butler, S. G., Telmer, P. G., Black, F. E., Renaud, J. B., & Sumarah, M. W. (2020). Identification and characterization of an aspergillus Niger amine oxidase that detoxifies intact Fumonisins. *Journal of Agricultural and Food Chemistry, 68*, 13779–13790. https://doi.org/10.1021/acs.jafc.0c04504

Gasser, K., Sulyok, M., Spangl, B., Krska, R., Steinkellner, S., & Hage-Ahmed, K. (2023). Fusarium proliferatum secondary metabolite profile in vitro depends on the origin of the isolates and is clearly reduced in stored garlic. *Postharvest Biology and Technology, 200*, Article 112312. https://doi.org/10.1016/j.postharvbio.2023.112312

Goessens, T., Mouchtaris-Michailidis, T., Tesfamariam, K., Truong, N. N., Vertriest, F., Bader, Y., … De Boevre, M. (2024). Dietary mycotoxin exposure and human health risks: A protocol for a systematic review. *Environment International, 184*, Article 108456. https://doi.org/10.1016/j.envint.2024.108456

Horai, H., Arita, M., Kanaya, S., Nihei, Y., Ikeda, T., Suwa, K., … Nishioka, T. (2010). MassBank: A public repository for sharing mass spectral data for life sciences. *Journal of Mass Spectrometry, 45*, 703–714. https://doi.org/10.1002/jms.1777

Huang, L., Song, Y., Li, N., Gao, J., Zhang, B., Liu, Z., & Zheng, Y. (2025). Deletion of bikaverin and fusarubin biosynthesis gene clusters via CRISPR/Cas9 system in fusarium fujikuroi and its effect on GA3 biosynthesis. *Journal of Biotechnology, 405*, 229–237. https://doi.org/10.1016/j.jbiotec.2025.06.004

Institute of Sciences of Food Production. (2025). *Agro-Food Microbial Culture Collection*. Retrieved July 29, 2025, from http://server.ispa.cnr.it/ITEM/Collection/ITEMCollection_Sx.php.

Jajić, I., Dudaš, T., Krstović, S., Krska, R., Sulyok, M., Bagi, F., Savić, Z., Guljaš, D., & Stankov, A. (2019). Emerging fusarium mycotoxins fusaproliferin, beauvericin, enniatins, and moniliformin in Serbian maize. *Toxins, 11*, 357. https://doi.org/10.3390/toxins11060357

Jestoi, M. (2008). Emerging fusarium-mycotoxins fusaproliferin, beauvericin, enniatins, and moniliformin - A review. *In Critical Reviews in Food Science and Nutrition, 48*, 21–49. https://doi.org/10.1080/10408390601062021

Kleigrewe, K., Söhnel, A. C., & Humpf, H. U. (2011). A new high-performance liquid chromatography-tandem mass spectrometry method based on dispersive solid phase extraction for the determination of the mycotoxin fusarin C in corn ears and processed corn samples. *Journal of Agricultural and Food Chemistry, 59*(19), 10470–10476. https://doi.org/10.1021/jf2026814

Knutsen, H. K., Åkesson, A., Bampidis, V., Bodin, L., Chipman, J. K., Degen, G., … Bignami, M. (2024). Genotoxicity of beauvericin. *EFSA Journal, 22*(10), Article e9031. https://doi.org/10.2903/j.efsa.2024.9031

Knutsen, H. K., Barregård, L., Bignami, M., Brüschweiler, B., Ceccatelli, S., Cottrill, B., … Alexander, J. (2018). Appropriateness to set a group health-based guidance value for fumonisins and their modified forms. *EFSA Journal, 16*(2), 5172. https://doi.org/10.2903/j.efsa.2018.5172

Kolawole, O., Meneely, J., Petchkongkaew, A., & Elliott, C. (2021). A review of mycotoxin biosynthetic pathways: Associated genes and their expressions under the influence of climatic factors. *In Fungal Biology Reviews, 37*, 8–26. Elsevier ltd https://doi.org/10.1016/j.fbr.2021.04.003.

Lale, G. J., & Gadre, R. V. (2016). Production of bikaverin by a fusarium fujikuroi mutant in submerged cultures. *AMB Express, 6*, 34. https://doi.org/10.1186/s13568-016-0205-0

Lazzaro, I., Busman, M., Battilani, P., & Butchko, R. A. E. (2012). FUM and BIK gene expression contribute to describe fumonisin and bikaverin synthesis in fusarium verticillioides. *International Journal of Food Microbiology, 160*, 94–98. https://doi.org/10.1016/j.ijfoodmicro.2012.10.004

Lazzaro, I., Falavigna, C., Galaverna, G., Dall'Asta, C., & Battilani, P. (2013). Cornmeal and starch influence the dynamic of fumonisin B, A and C production and masking in fusarium verticillioides and F. Proliferatum. *International Journal of Food Microbiology, 166*, 21–27. https://doi.org/10.1016/j.ijfoodmicro.2013.06.011

Li, T., Li, J., Wang, J., Xue, K. S., Su, X., Qu, H., … Jiang, Y. (2024). The occurrence and management of fumonisin contamination across the food production and supply chains. *In Journal of Advanced Research, 60*, 13–26. Elsevier B.V. https://doi.org/10.1016/j.jare.2023.08.001

Limón, M. C., Rodríguez-Ortiz, R., & Avalos, J. (2010). Bikaverin production and applications. *Applied Microbiology and Biotechnology, 87*, 21–29. https://doi.org/10.1007/s00253-010-2551-1

Logrieco, A., & Moretti, A. (1995). Occurrence and toxigenicity of fusarium proliferatum from preharvest maize ear rot, and associated mycotoxins, in Italy. *Plant Disease, 79*, 727–731.

Lu, H., Guo, S., Yang, Y., Zhao, Z., Xie, Q., Wu, Q., Sun, C., Luo, H., An, B., & Wang, Q. (2025). Bikaverin as a molecular weapon: Enhancing fusarium oxysporum

pathogenicity in bananas via rhizosphere microbiome manipulation. *Microbiome, 13*, 107. https://doi.org/10.1186/s40168-025-02109-7

Matsuo, Y., Takahara, K., Sago, Y., Kushiro, M., Nagashima, H., & Nakagawa, H. (2015). Detection of N-(1-deoxy-d-fructos-1-yl) fumonisins B2 and B3 in corn by high-resolution LC-Orbitrap MS. *Toxins, 7*, 3700–3714. https://doi.org/10.3390/toxins7093700

Molnár, A., Knapp, D. G., Lovas, M., Tóth, G., Boldizsár, I., Váczy, K. Z., & Kovács, G. M. (2023). Untargeted metabolomic analyses support the main phylogenetic groups of the common plant-associated Alternaria fungi isolated from grapevine (*Vitis vinifera*). *Scientific Reports, 13*, 19298. https://doi.org/10.1038/s41598-023-46020-3

Moretti, A., Logrieco, A., Bottalico, A., Ritieni, A., Fogliano, V., & Randazzo, G. (1996). Diversity in beauvericin and fusaproliferin production by different populations of Gibberella fujikuroi (fusarium section Liseola). *Sydowia, 48*, 44–56.

Munkvold, G. P., Proctor, R. H., & Moretti, A. (2021). Mycotoxin production in fusarium according to contemporary species concepts. *Annual Review of Phytopathology, 59*, 373–402. https://doi.org/10.1146/annurev-phyto-020620-102825

Musser, S. M., Eppley, R. M., Mazzola, E. P., Hadden, C. E., Shockcor, J. P., Crouch, R. C., & Martin, G. E. (1995). Identification of an N-acetyl keto derivative of fumonisin B1 in corn cultures of fusarium proliferatum. *Journal of Natural Products, 58*(9), 1392–1397. https://pubs.acs.org/sharingguidelines.

Musser, S. M., & Plattner, R. D. (1997). Fumonisin composition in cultures of fusarium moniliforme, fusarium proliferatum, and fusarium nygami. *Journal of Agricultural and Food Chemistry, 45*, 1169–1173. https://pubs.acs.org/sharingguidelines.

Niehaus, E. M., Münsterkötter, M., Proctor, R. H., Brown, D. W., Sharon, A., Idan, Y., … Tudzynski, B. (2016). Comparative "omics" of the fusarium fujikuroi species complex highlights differences in genetic potential and metabolite synthesis. *Genome Biology and Evolution, 8*(11), 3574–3599. https://doi.org/10.1093/gbe/evw259

Nielsen, E., Egebjerg, M. M., Olesen, T., Sharma, A. K., Nørby, K., Beltoft, V., … Jørgensen, K. (2018). *Extensive literature search for studies related to fumonisins and their modified forms*. https://doi.org/10.2903/sp.efsa.2018.EN-1148

Nothias, L. F., Petras, D., Schmid, R., Dührkop, K., Rainer, J., Sarvepalli, A., … Dorrestein, P. C. (2020). Feature-based molecular networking in the GNPS analysis environment. *Nature Methods, 17*, 905–908. https://doi.org/10.1038/s41592-020-0933-6

Poynton, E. F., Van Santen, J. A., Pin, M., Contreras, M. M., McMann, E., Parra, J., … Linington, R. G. (2025). The natural products atlas 3.0: Extending the database of microbially derived natural products. *Nucleic Acids Research, 53*, D691–D699. https://doi.org/10.1093/nar/gkae1093

Proctor, R. H., Busman, M., Seo, J. A., Lee, Y. W., & Plattner, R. D. (2008). A fumonisin biosynthetic gene cluster in fusarium oxysporum strain O-1890 and the genetic basis for B versus C fumonisin production. *Fungal Genetics and Biology, 45*, 1016–1026. https://doi.org/10.1016/j.fgb.2008.02.004

Proctor, R. H., Desjardins, A. E., & Moretti, A. (2010). Biological and chemical complexity of fusarium proliferatum. In R. N. Strange, & M. L. Gullino (Eds.), *The role of plant pathology in food safety and food security* (pp. 97–111). Springer. https://doi.org/10.1007/978-1-4020-8932-9_9.

Rabaaoui, A., Dall'Asta, C., Righetti, L., Susca, A., Logrieco, A. F., Namsi, A., … Masiello, M. (2021). Phylogeny and mycotoxin profile of pathogenic fusarium species isolated from sudden decline syndrome and leaf wilt symptoms on date palms (*Phoenix dactylifera*) in Tunisia. *Toxins, 13*, 463. https://doi.org/10.3390/toxins13070463

Renaud, J. B., Desrochers, N., Hoogstra, S., Garnham, C. P., & Sumarah, M. W. (2021). Structure activity relationship for Fumonisin Phytotoxicity. *Chemical Research in Toxicology, 34*, 1604–1611. https://doi.org/10.1021/acs.chemrestox.1c00057

Righetti, L., Bergmann, A., Galaverna, G., Rolfsson, O., Paglia, G., & Dall'Asta, C.. (2018). Ion mobility-derived collision cross section database: Application to mycotoxin analysis. *Analytica Chimica Acta, 1014*, 50–57. https://doi.org/10.1016/j.aca.2018.01.047

Righetti, L., Dreolin, N., Celma, A., McCullagh, M., Barknowitz, G., Sancho, J. V., & Dall'Asta, C.. (2020). Travelling wave ion mobility-derived collision cross section for mycotoxins: Investigating interlaboratory and interplatform reproducibility. *Journal of Agricultural and Food Chemistry, 68*, 10937–10943. https://doi.org/10.1021/acs.jafc.0c04498

Righetti, L., Paglia, G., Galaverna, G., & Dall'Asta, C.. (2016). Recent advances and future challenges in modified mycotoxin analysis: Why HRMS has become a key instrument in food contaminant research. In *, Vol. 8. Toxins* (p. 361). MDPI AG. https://doi.org/10.3390/toxins8120361.

Ross, D. H., Cho, J. H., & Xu, L. (2020). Breaking down structural diversity for comprehensive prediction of ion-neutral collision cross sections. *Analytical Chemistry, 92*, 4548–4557. https://doi.org/10.1021/acs.analchem.9b05772

Rychlik, M., Humpf, H. U., Marko, D., Dänicke, S., Mally, A., Berthiller, F., … Lorenz, N. (2014). Proposal of a comprehensive definition of modified and other forms of mycotoxins including "masked" mycotoxins. *Mycotoxin Research, 30*, 197–205. https://doi.org/10.1007/s12550-014-0203-5

Salem, M. A., Jüppner, J., Bajdzienko, K., & Giavalisco, P. (2016). Protocol: A fast, comprehensive and reproducible one-step extraction method for the rapid preparation of polar and semi-polar metabolites, lipids, proteins, starch and cell wall polymers from a single sample. *Plant Methods, 12*(45). https://doi.org/10.1186/s13007-016-0146-2

Santos, M. C. D., Mendonça, M. D. L., & Bicas, J. L. (2020). Modeling bikaverin production by fusarium oxysporum CCT7620 in shake flask cultures. *Bioresources and Bioprocessing, 7*, 13. https://doi.org/10.1186/s40643-020-0301-5

Schneiders, A. L., Far, J., Belova, L., Fry, A., Covaci, A., Baker, E. S., … Eppe, G. (2025). Structural characterization of dimeric perfluoroalkyl carboxylic acid using experimental and theoretical ion mobility spectrometry analyses. *Journal of the American Society for Mass Spectrometry, 36*, 850–861. https://doi.org/10.1021/jasms.5c00007

Schymanski, E. L., Jeon, J., Gulde, R., Fenner, K., Ruff, M., Singer, H. P., & Hollender, J. (2014). Identifying small molecules via high resolution mass spectrometry: Communicating confidence. In. *Environmental Science and Technology, 48*, 2097–2098. https://doi.org/10.1021/es5002105

Seefelder, W., Hartl, M., & Humpf, H. U. (2001). Determination of N-(carboxymethyl) fumonisin B1 in corn products by liquid chromatography/electrospray ionization-mass spectrometry. *Journal of Agricultural and Food Chemistry, 49*(5), 2146–2151. https://doi.org/10.1021/jf001429c

Seiferlein, M., Humpf, H. U., Voss, K. A., Sullards, M. C., Allegood, J. C., Wang, E., & Merrill, A. H. (2007). Hydrolyzed fumonisins HFB1 and HFB2 are acylated in vitro and in vivo by ceramide synthase to form cytotoxic N-acyl-metabolites. *Molecular Nutrition & Food Research, 51*(9), 1120–1130. https://doi.org/10.1002/mnfr.200700118

Selegato, D. M., Zanatta, A. C., Pilon, A. C., Veloso, J. H., & Castro-Gamboa, I. (2023). Application of feature-based molecular networking and MassQL for the MS/MS fragmentation study of depsipeptides. *Frontiers in Molecular Biosciences, 10*. https://doi.org/10.3389/fmolb.2023.1238475

Shannon, P., Markiel, A., Ozier, O., Baliga, N. S., Wang, J. T., Ramage, D., … Ideker, T. (2003). Cytoscape: A software environment for integrated models of biomolecular interaction networks. *Genome Research, 13*(11), 2498–2504. https://doi.org/10.1101/gr.1239303

Shi, W., Tan, Y., Wang, S., Gardiner, D. M., De Saeger, S., Liao, Y., … Wu, A. (2017). Mycotoxigenic potentials of fusarium species in various culture matrices revealed by mycotoxin profiling. *Toxins, 9*, 6. https://doi.org/10.3390/toxins9010006

Tagyan, A. I., AlAshaal, S., Alkhalifah, D. H. M., Abdelghany, W. R., & Hozzein, W. N. (2025). Estimating the climate change-driven global distribution of fusarium proliferatum and mycotoxin risk assessment under future warming scenarios. *Frontiers in Forests and Global Change, 8*, Article 1673494. https://doi.org/10.3389/ffgc.2025.1673494

Tamura, M., Mochizuki, N., Nagatomi, Y., Toriba, A., & Hayakawa, K. (2014). Characterization of fumonisin A-series by high-resolution liquid chromatography-orbitrap mass spectrometry. *Toxins, 6*, 2580–2593. https://doi.org/10.3390/toxins6082580

The Commission of the European Communities. (2006). Commission regulation (EC) no 1881/2006 of 19 December 2006 setting maximum levels for certain contaminants in foodstuffs. *Official Journal of the European Union, L, 364*, 5.

Tolosa, J., Serrano Candelas, E., Vallés Pardo, J. L., Goya, A., Moncho, S., Gozalbes, R., & Palomino Schätzlein, M. (2023). MicotoXilico: An interactive database to predict mutagenicity, genotoxicity, and carcinogenicity of mycotoxins. *Toxins, 15*, 355. https://doi.org/10.3390/toxins15060355

Urbaniak, M., Stępień, Ł., & Uhlig, S. (2019). Evidence for naturally produced beauvericins containing N-methyl-tyrosine in Hypocreales Fungi. *Toxins, 11*, 182. https://doi.org/10.3390/toxins11030182

Urbaniak, M., Waśkiewicz, A., Trzebny, A., Koczyk, G., & Stępień, Ł. (2020). Cyclodepsipeptide biosynthesis in hypocreales fungi and sequence divergence of the non-ribosomal peptide synthase genes. *Pathogens, 9*, 552. https://doi.org/10.3390/pathogens9070552

Witte, T. E., Hermans, A., Sproule, A., Hicks, C., Talhouni, T., Schneiderman, D., … Overy, D. P. (2024). Identification and confirmation of virulence factor production from fusarium avenaceum, a causal agent of root rot in pulses. *Journal of Fungi, 10*, 821. https://doi.org/10.3390/jof10120821

Witte, T. E., Villenueve, N., Shields, S. W., Sproule, A., Eggertson, Q., Kim, N. E., … Overy, D. P. (2022). Untargeted metabolomics screening reveals unique secondary metabolite production from Alternaria section Alternaria. *Frontiers in Molecular Biosciences*. https://doi.org/10.3389/fmolb.2022.1038299

Wolf, S., Schmidt, S., Müller-Hannemann, M., & Neumann, S. (2010). In silico fragmentation for computer assisted identification of metabolite mass spectra. *BMC Bioinformatics, 11*, 148. https://doi.org/10.1186/1471-2105-11-148

World Health Organization. (2015). WHO estimates of the global burden of foodborne diseases : Foodborne disease burden epidemiology reference group 2007-2015. *World Health Organization*.

World Health Organization. International Agency for Research on Cancer. (2002). IARC monographs on the evaluation of carcinogenic risks to humans. In *, 82. Some Traditional Herbal Medicines, Some Mycotoxins, Naphthalene and Styrene*. IARCPress.

Xu, X., Zhao, S., Yu, Y., Chen, Z., Shen, H., & Zhou, L. (2016). Beauvericin K, a new antifungal Beauvericin analogue from a marine-derived fusarium sp. *Natural Product Communications, 11*, 1825–1826.

Yu, S., Jia, B., Liu, N., Yu, D., Zhang, S., & Wu, A. (2021). Fumonisin B1 triggers carcinogenesis via HDAC/PI3K/Akt signalling pathway in human esophageal epithelial cells. *Science of the Total Environment, 787*, Article 147405. https://doi.org/10.1016/j.scitotenv.2021.147405

Zhang, H., Luo, M., Wang, H., Ren, F., Yin, Y., & Zhu, Z.-J. (2023). AllCCS2: Curation of ion mobility collision cross-cection atlas for small molecules using comprehensive molecular representations. *Analytical Chemistry, 95*, 13913–13921. https://doi.org/10.1021/acs.analchem.3c02267

Zhang, T., Zhuo, Y., Jia, X. P., Liu, J. T., Gao, H., Song, F. H., … Zhang, L. X. (2013). Cloning and characterization of the gene cluster required for beauvericin biosynthesis in fusarium proliferatum. *Science China Life Sciences, 56*(7), 628–637. https://doi.org/10.1007/s11427-013-4505-1